

ABSTRACT

The aim of this work is the evaluation and the analysis of the different chemical-physical variables that affect the emission of volatile organic compounds (VOC) and odours from passive liquid area sources inside a wind tunnel, which is typically used for emission sampling. Three different compounds (acetone, butanol and ethanol), having different volatilization properties (e.g., boiling point, solubility), were studied in solution with water at different concentrations. The following physical parameters affecting the VOC volatilization in the Wind Tunnel system were evaluated: the velocity of the air flowing through the device, in a range from 0.01 to about 0.05 m/s, and the temperature of both the liquid source and the sweep air flow, in a range from 12°C to 42°C. The experimental results were compared with the existing volatilization models available in literature. In most cases the proposed theoretical model predicts well the experimentally measured concentration. Some discrepancies were observed for lower velocities and also by moving from the room temperature (20° C); and those were discussed by making some considerations about the volatilization phenomenon. Moreover, the study clearly shows that it is not the gas phase temperature that controls the emission, but the temperature of the liquid phase, due to the effect of the latter on the vapour pressure of the compound, which is the main driving force of the phenomenon.

1. INTRODUCTION

The establishment or enlargement of residential areas close to industrial sites has caused the growth of a new air quality issue, that is odour pollution (Yuwono and Lammers, 2004). It has been demonstrated that even at very low concentrations people can detect the presence of malodorous volatile organic compounds (VOC) (Laska and Hudson, 1991; Leonardos et al., 1969) , which may in some cases cause negative effects on their well-being (Hayes et al., 2017; Schiffman et al., 1995; Van Harreveld, 2001).

25 Therefore, in recent years, different European governments have issued new regulations related to
26 odour emissions and olfactory discomfort. Big efforts have been made especially in the
27 standardization of methods for the objective quantification of odour emissions. The European Norm
28 13725:2003, which standardizes the measurement of the so called “odour concentration” by
29 dynamic olfactometry, also gives some indications about the sampling methods to be adopted for
30 the different types of odour sources. For passive liquid area sources, such as wastewater
31 treatment tanks, which represent in a lot of cases an important source of odour pollution and
32 complaints, odour emission assessment is very difficult and – up to now - there is still no straight-
33 forward nor established sampling procedure (Capelli et al., 2013). The methods that are most
34 commonly applied for odour emission assessment on passive area sources are the so called “hood
35 methods”, whereby a sort of enclosure is placed on the emission surface and air is blown through it
36 to simulate the wind action over the monitored surface (Beghi et al., 2012; Bliss et al., 1995;
37 Capelli et al., 2009; Gostelow et al., 2003; Hudson and Ayoko, 2008). Among “hood methods”,
38 Wind Tunnels (WT) are widely used in many countries (Bliss et al., 1995; Ryden and Lockyer,
39 1985; Smith and Watts, 1994). In such systems, a sweep air flow parallel to the emitting surface is
40 applied (Capelli et al., 2013, 2009; Frechen et al., 2004; Parker et al., 2010). With Wind Tunnels,
41 the assessment of the odour emission rate (OER) involves three phases: on-site sampling (Capelli
42 et al., 2009; Koziel et al., 2005), sample analysis (CEN, 2003) and data elaboration. Data
43 elaboration is necessary in order to evaluate the Specific Odour Emission Rate (SOER), expressed
44 in odour units emitted from the source per surface and time unit [$\text{ou}/\text{m}^2/\text{s}$], from the odour
45 concentration that is the direct outcome of the olfactometric measurement. Moreover, for the
46 purpose of emission assessment, the SOER must be referred to the neutral sweep air flow rate
47 used during sampling (Capelli et al., 2009).

48 While researchers have analysed and modelled the volatilization of different VOC in the open field
49 (Kawamura and Mackay, 1987; Sutton, 1934), these models cannot be applied as such to evaluate
50 odour emissions. Environmental odours typically are complex mixtures with unknown composition,
51 comprising hundreds of compounds having different physical and chemical properties, often in
52 aqueous solution, and thus different volatilization behaviours. This is the reason why, for odour

53 emission assessment purposes, experimental data shall be retrieved case by case for source
54 characterization, giving that field sampling becomes a crucial issue. However, the literature about
55 the volatilization inside the WT is very poor. Hudson and Ayoko, 2008 have highlighted that there
56 are many different parameters having a strong influence on this phenomenon, such as WT
57 geometry and dimensions, nature of VOC, temperature, and air velocity.

58 The aim of this work is to investigate the major factors affecting the volatilization of VOC from liquid
59 area sources and analyse their effect in order to develop an effective model to describe
60 volatilization inside the hood.

61 **1.1. STATE-OF-THE-ART: WIND TUNNEL VOLATILIZATION MODELS**

62 Different models exist in literature for describing liquid-gas mass transfer. A recent paper by (Prata
63 A.A. et al., 2018) presents an extensive review of models for the mass transfer coefficients both on
64 the gas and liquid phase. However, up to now, no general model has been proposed accounting
65 for all the different situations that might take place inside the Wind Tunnel and affect the
66 volatilization phenomenon. The models available in literature are sometimes scarcely reliable and
67 affected by strong approximations. Below, two models are reported, which are the most
68 representative for the case under investigation and were therefore considered for this study.

69 **1.1.1. Model for single flat emissive surface (modified)**

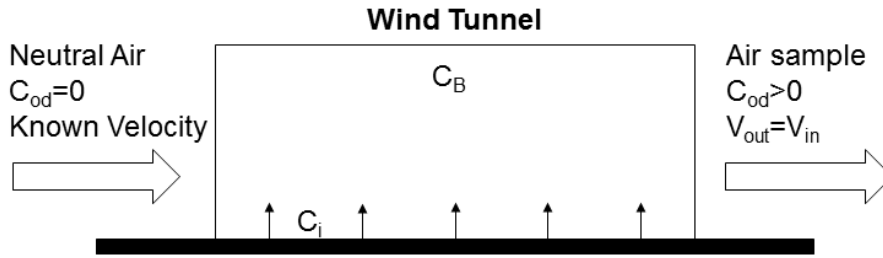
70 Lucernoni et al., 2017 developed the following model to describe volatilization of pure compounds
71 inside the Wind Tunnel system. It is based on the Prandtl boundary layer theory (Incropera and
72 DeWitt, 2002), according to the hypothesis that mass transfer under forced convection over a
73 single flat emissive surface in laminar regime can properly approximate the conditions inside the
74 Wind Tunnel.

75 The main contributors for the mass transfer is due to the gas motion just above the emitting
76 surface, instead of the chemical diffusion. Therefore, in order to compute the coefficient for

77 convective mass transfer, it is possible to use the correlation for the mass transfer from a single flat
 78 emitting surface:

$$79 \quad K_{c,ave} = 0.664 \left(\frac{D_{i,air}^4}{L_{WT}^3 \nu} \right)^{\frac{1}{6}} u_{WT}^{1/2} \quad (1)$$

80 Where: $D_{i,air}$ is the compound molecular diffusivity in air in [m²/s]; L_{WT} is the length of the WT
 81 central body in [m]; ν is the air kinematic viscosity in [m²/s]; u_{WT} is the air velocity inside the hood in
 82 [m/s].



83

84 *Figure 1. Simplified scheme for the wind tunnel system, according to the model of Lucernoni et al. (2017) [1 column*
 85 *fitting image]*

86 The following step involves the mass balance on the system, between the inlet and the outlet of the
 87 WT:

$$88 \quad Q \cdot C_{out} = Q \cdot C_{in} + K_{c,ave} \cdot (C_i - C_B)A \quad (2)$$

89 Where: Q is the neutral air flow rate blown in the WT in [m³/s]; C_{out} is the compound concentration
 90 at the outlet in [mol/m³]; C_{in} is the compound concentration at the inlet in [mol/m³], that is null if
 91 neutral air is used; $K_{c,ave}$ is the convective mass transfer coefficient averaged over the exchange
 92 length, in [m/s]; A is the base area of the WT in [m²]. According to Lucernoni et al. (2017), it is the
 93 diffusion in the gas-film close to the interface (boundary layer) that affects the exchange rate. Thus,
 94 the gas-liquid interface concentration of the compound C_i in [mol/m³] coincides with the
 95 concentration in the gas side of the gas-liquid interface, and is computed as follows:

96

$$C_i = \frac{P_{sat}(T_{liq})}{R * T_{liq}} \quad (3)$$

97 Where: $P_{sat}(T_{liq})$ is the vapour pressure of the compound, computed at the liquid temperature [Pa];
98 R is the universal gas constant equal to 8.314 [J/mol/K]; T_{liq} is the temperature of the liquid phase
99 [K].

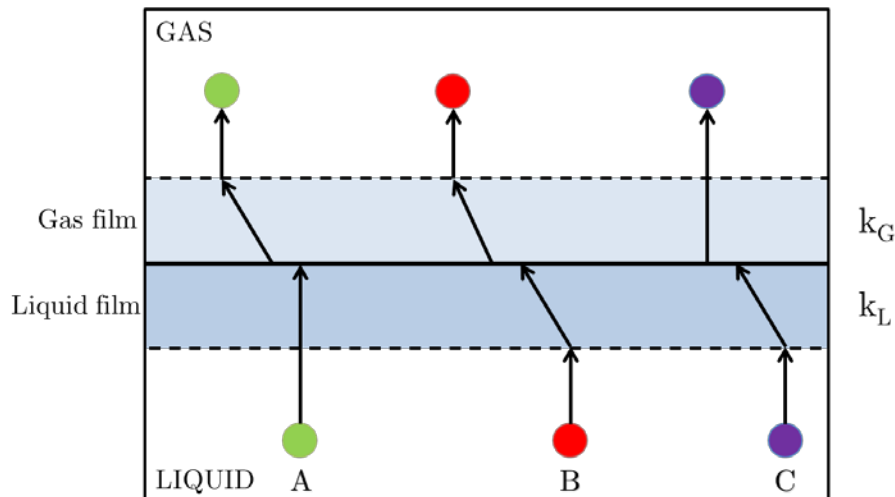
100 In this case, we didn't consider the classical single flat plate model, for which C_B , i.e. the compound
101 concentration in the bulk of the gas phase inside the hood in [mol/m³], is equal to the inlet
102 concentration (in this case equal to zero since neutral air is used). A slight modification to this
103 classical model was introduced in order to account for the particular geometry studied, thus making
104 the same assumptions as in Lucernoni et al. (2017), who used the same kind of sampling hood.
105 For this reason, according to Lucernoni et al. (2017), C_B , can be assumed equal to 50% of the
106 outlet concentration, thus considering it as the average between inlet and outlet concentrations
107 with a 0 inlet concentration:.

108

$$C_{out} = \frac{K_{c,ave} C_i A}{\left(Q + \frac{K_{c,ave} A}{2}\right)} \quad (4)$$

109 **1.1.2. The two-film model**

110 Parker et al. (2010) proposed a model for liquid mixtures, which was verified experimentally, and
111 which takes into account two different factors that may affect the volatilization of compounds from
112 liquid area sources: the air velocity and the Henry constant (strongly influenced by temperature).
113 Several researchers have used the conventional two-film model for their studies on mass transport
114 (Bianchi and Varney, 1997; Liss and Slater, 1974; Whitman, 1962).



115

116 *Figure 2. Conceptual scheme for the two-film model, representing the path of a gas-phase controlled molecule (A), an*
 117 *intermediate molecule (B) and a liquid-film controlled molecule (C). [1 column fitting image]*

118 At the basis of this model there is the assumption that a VOC molecule moving from the liquid
 119 phase to the gas phase must pass through two different films: i.e. the liquid film and the gas film.
 120 Some molecules can experience a stronger resistance in one of the two films or even in both of
 121 them, as illustrated in Figure 2:

- 122 • Gas phase controlled molecules have a stronger resistance to the transport while
 123 passing through the gas film, and they follow the path of molecule A in the figure.
- 124 • Liquid phase controlled compounds face a major resistance in the liquid film and
 125 conceptually they follow the path of molecule C.
- 126 • The compounds that are neither gas phase controlled nor liquid phase controlled follow
 127 the path of molecule B.

128 The volatilization flux according to this model can be written as follows:

129
$$J = k_L (C_L - C_L^*) = k_G (C_G^* - C_G) \quad (5)$$

130 where J is the flux [$\text{kg}/\text{m}^2/\text{s}$], k_L is the liquid-film transfer coefficient [m/s], k_G is the gas-film transfer
 131 coefficient [m/s], C_L is the VOC concentration in the liquid phase [kg/m^3], C_G is the VOC
 132 concentration in the vapour phase [kg/m^3], C_L^* is the VOC concentration in the liquid side of gas-

133 liquid interface [kg/m^3], and C_G^* is the VOC concentration in the gas side of gas-liquid interface
134 [kg/m^3].

135

136 1.2. **General models for volatilization inside Wind Tunnels**

137 As previously mentioned, different models exist in literature for describing liquid-gas mass transfer
138 (Prata A.A. et al., 2018) ; however, models accounting for the effect of the different variables
139 evaluated in this study are limited in literature. Furthermore, there are fewer studies regarding the
140 behaviour of aqueous solutions of volatile compounds compared to pure compounds.

141 However, several researchers have highlighted the importance of temperature and humidity in
142 volatilization processes. Montes et al., 2010; Parker et al., 2010; Raimundo et al., 2014 analysed
143 the evaporation of water inside a WT system by changing the operating conditions inside it (i.e.
144 temperature, relative humidity and velocity of the sweep air flow); they elaborated their data to
145 evaluate the evaporating flux from the tank and then compared it with different expressions
146 available in literature. At the end, they also developed their own equation for the evaporating flux,
147 which includes the different factors they had evaluated in their trial. Even if their study regarded a
148 pure compound (water), it is very interesting, since they were able to develop a first equation
149 accounting for all the parameters that were investigated also in our study, giving that it can be
150 considered as an initial step for further developments in this field. In the present study, the
151 influence of the humidity of the sweep air flow rate was not analysed: this because the aim here is
152 to study the influence of the emission of organic compound in solution and not a pure water
153 emission.

154 2. MATERIALS AND METHODS

155 2.1. Theoretical model

156 In this study we investigated the emission mechanism inside the wind tunnel. In this case, it was
157 decided to evaluate the emission from an aqueous solution to have a situation much more similar
158 to the real emitting situations, like in WWTPs.

159 Differently from the pure compound configuration, studied by (Lucernoni et al., 2017), in this case
160 two different films affecting the transport phenomena shall be considered: the liquid film and the
161 gas film, as illustrated for the case of molecule B in Figure 2.

162 Eq. 5 can still be assumed as valid, considering that the hypothesis of steady state mass transfer
163 at the interface is still applicable. Since the measure of the concentration at the two side of the
164 interface is not possible, equilibrium across the interface is assumed, giving that C_G^* and C_L^* lie on
165 the equilibrium curve, and:

$$166 \quad C_G^* = f(C_L^*) \quad (6)$$

167 To describe the rate of interface transport there are two different ways. The former is to use
168 Equation 5 and 6 to calculate the interface concentration and then use the single phase mass
169 transfer coefficients (k_G and k_L). The latter, and more used in literature (Bird, 2002; Thibodeaux
170 and Mackay, 2010), is to introduce overall mass transfer coefficients by introducing equilibrium
171 concentrations as:

$$172 \quad J = K_L (C_L - C_L^{eq}) = K_G (C_G^{eq} - C_G) \quad (7)$$

173 Where C_L^{eq} is a liquid concentration in equilibrium with the bulk vapour concentration C_G (i.e.,
174 $C_L^{eq} = f(C_G)$), C_G^{eq} is a vapour concentration in equilibrium with the bulk liquid concentration C_L (i.e.,
175 $C_G^{eq} = f(C_L)$), while K_L and K_G are the overall mass transfer coefficients, which will be clarified later.

176 The main advantage of Equation 7 is that it is function of experimentally evaluable concentrations,
177 i.e., C_G and C_L .

178 In the following part of the discussion it was decided to use the relation relevant to the liquid mass
179 transfer:

$$180 \quad J = K_L (C_L - f(C_G)) \quad (8)$$

181 The values for the mass transport coefficients for the two films are computed by means of
182 equations recovered from literature. It is important to highlight that, for the liquid film the correlation
183 is independent from the air velocity. This is only true in the case of static situations, in which the air
184 flow does not induce movement on the liquid surface. For situations in which the fluid elements
185 close to the surface are moving or in which the surface is not properly “quiescent”, because of the
186 generation of waves due to the wind action, different models should be adopted (Prata et al.,
187 2017).

188 On the other hand, for gas phase controlled compounds, there is a strong dependence from this
189 factor, since the volatilization is mainly connected to forced convection.

190 For the gas film side, the considerations made by Lucernoni et al. (2017) are still valid. So, to
191 evaluate the gas film coefficient, the following equation can be established, derived from Eq. (1):

$$192 \quad k_G = 0.664 \left(\frac{D_{i,air}^4}{L_{WT}^3 v} \right)^{\frac{1}{6}} u_{WT}^{1/2} \quad (9)$$

193 Where k_G [m/s], is the gas film coefficient considered for the theoretical model of this work.

194 On the other side, for the liquid side exchange coefficient, for completely static liquid
195 configurations, the Higbie penetration theory should be used (Cussler, 2009). In this case the
196 transport coefficient for the liquid phase should be evaluated with the following equation:

$$197 \quad k_L = \frac{2}{\sqrt{\pi}} \left(\frac{D_{i,H_2O}}{t_s} \right)^{\frac{1}{2}} \quad (10)$$

198 Where k_L [m/s] is the mass transfer coefficient for the liquid film, D_{i, H_2O} [m²/s] is the diffusion
199 coefficient of the compound in water, t_s is the sampling time [s].

200 By using the approach of Equation 7 and considering negligible the contribution of Poynting
201 correction, by working at atmospheric pressure, the relation among C_G and C_L^{eq} can be evaluated
202 through the Raoult's modified law (Carroll, 1991):

$$203 \quad C_G = \frac{P_i^\circ(T) \cdot \gamma_i}{RT C_L^{TOT}} C_L^{eq} \quad (11)$$

204 Where $P_i^\circ(T)$ [Pa] is the vapour pressure of the solute in the experimental conditions, R is the gas
205 constant [J/mol K], T [K] the temperature, γ_i [-] the activity coefficient of the compound in solution,
206 and C_L^{TOT} the liquid total molar concentration [mol/m³].

207 Of course, for diluted solutions it is not trivial to consider the Henry's Law as representative of the
208 equilibrium situation, which is the approach more frequently found in literature. Eq. (12) reports the
209 definition of Henry's constant (Smith et al., 2007):

$$210 \quad H_i = \lim_{x_i \rightarrow 0} \frac{f_i}{x_i} \quad (12)$$

211 Where f_i [-] and x_i [-] are the fugacity and the mole fraction of the solute in water. By means of this
212 equation, it is easy to understand that the Henry's law is valid when the fraction of the organic
213 compound is close to zero, i.e. in the case of diluted solutions.

214 In these case, the following equation can be adopted, and considering the volatilization formula
215 (Sander, 2015), Eq. (13) could be used:

$$216 \quad C_G^{eq} = K_H^{CC} \cdot C_L^{eq} \quad (13)$$

217 where K_H^{CC} is the dimensionless Henry's law constant, defined as:

$$218 \quad K_H^{CC} = \frac{1}{H^{cp} \cdot RT} \quad (14)$$

219 Where H^{fp} [mol/m³Pa] is the solubility Henry's constant, R is the gas constant, T [K] the
220 temperature (for more detail about Henry's law and constants see Sander, 2015).

221 The Henry's law constant is fundamental for example in Parker's work (Parker et al., 2010), since it
222 is the major discriminant for the classification of the different compounds: for K_H^{CC} values lower
223 than 1×10^{-3} the main resistance to transport is located in the gas film (gas phase controlled); if K_H^{CC}
224 is higher than 1×10^{-1} the compounds are liquid phase controlled; for intermediate values, both of
225 the phases have a strong influence on the volatilization process (Hudson and Ayoko, 2008). In the
226 same paper, Parker enlists a series of the main VOC with their values of the dimensionless Henry
227 constant and divides them into the three different categories.

228 To compare the experimental results of our trials with the theoretical model, the mole fraction of 0.1
229 was stated as limit between the two equilibrium models: if the mole fraction of the compound in
230 solution was smaller than 0.1, Henry's law (Eq. (13)) was used, even though the Raoult's modified
231 law is always valid along the whole range of mole fractions. Otherwise, if mole fraction was greater
232 than 0.1, Raoult's modified law was preferred (Eq. (11)). The numerical values of these parameters
233 were obtained in different ways: Henry's constants were taken from the most recent results
234 reported in Sander (2015); for the evaluation of the activity coefficients the free available online
235 AIOMFAC model (Zuend et al., 2011) was used.

236 Despite the different thermodynamical model used to describe equilibrium, by rearranging with few
237 calculus passages and considering the ideal gas law, it is possible to identify a unique equation to
238 describe the equilibrium at the interface as:

239
$$C_G^{eq} = \Lambda_{eq} \cdot C_L^{eq} \quad (15)$$

240 Where Λ_{eq} [-] is the equilibrium constant deriving from Eq. (11) or Eq. (13) for each situation.

241 Through this correlation, it is possible to evaluate the overall mass flux and the relative coefficient:

242
$$J = K_L \left(C_L - \frac{C_G}{\Lambda_{eq}} \right) \quad (16)$$

243
$$K_L = \frac{k_L k_G \Lambda_{eq}}{k_G \Lambda_{eq} + k_L} \quad (17)$$

244 Where J is the specific flux [kg/m²/s], K_L [m/s] is the overall mass transfer coefficient, C_L and C_G
 245 [mol/m³] are the concentrations of the VOC respectively in the bulk liquid and bulk vapour phase
 246 and Λ_{eq} [-] the equilibrium constant.

247 By knowing the volatilization flux contribution, and considering the wind tunnel configuration as
 248 reported in Figure 1, it is then possible to write the mass balance for the hood:

249
$$Q \cdot C_{out} = Q \cdot C_{in} + K_L \cdot \left(C_L - \frac{C_G}{\Lambda_{eq}} \right) A \quad (18)$$

250 Where Q [m³/s] is the neutral air flow rate blown in the WT, C_{out} and C_{in} [mol/m³] are respectively
 251 the compound concentrations at the outlet and at the inlet of the hood, K_L [m/s] is the global mass
 252 transfer coefficient, which can be calculated by Eq. (17), C_L and C_G [mol/m³] are the concentrations
 253 of the compound respectively in the bulk liquid and bulk gas phase, Λ_{eq} [-] the equilibrium constant,
 254 and A [m²] is the base area of the WT.

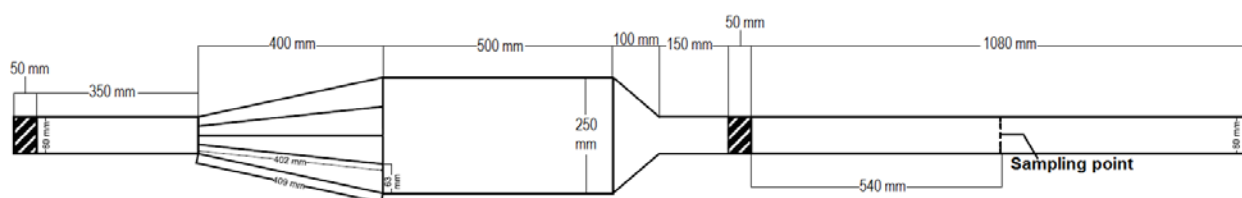
255 As previously mentioned, for the evaluation of the concentration in the bulk phase the same
 256 assumptions as in Lucernoni et al. (2017) were made: due to the specific geometry of the wind
 257 tunnel considered, the bulk concentration was set equal to the average between inlet and outlet
 258 concentrations, with $C_{in}=0$. ($C_G=C_{out}/2$). By this assumption, the outlet concentration can be
 259 evaluated as:

260
$$C_{out} = \frac{K_L \cdot A \cdot C_L}{Q_{out} + \frac{K_L \cdot A}{2 \Lambda_{eq}}} \quad (19)$$

261 This theoretical model was used for comparison with all the experimental results obtained in the
 262 laboratory tests.

263 2.2. Experimental setup

264 The WT used for this work was designed and developed by the Olfactometric Laboratory at
265 Politecnico di Milano. The structure of the hood is described in detail by Capelli et al. (2009), and is
266 schematically illustrated in Figure 3. It is the same WT used by Lucernoni in his work (2017). The
267 central body has a 25x50 cm base section and is 8 cm high. The hood has an open bottom to be
268 placed over the emissive surface. It has two converging sections at the extremes, connected to the
269 inlet and outlet. The WT is made of PVC and can be equipped with floating parts that allow
270 sampling on liquid sources.



271

272 *Figure 3. Wind tunnel scheme. [1 column fitting image]*

273 In order to better understand the volatilization phenomenon in the WT, it was decided to perform a
274 set of experiments with different compounds, in diluted solution with water (e.g. acetone, ethanol
275 and n-butanol).

276 The compounds were chosen due to their high volatility and possibility to be detected by a GC-FID.
277 Details about the analytic method are reported in the Supplementary Material (SM1).

278 For the tests, a small polyethylene tank exactly fitting the WT central body, filled with the liquid,
279 with a depth of 5 cm, was placed under the hood. Three sets of different experiments were
280 performed, whereby for each set of experiments a different parameter was evaluated (velocity, and
281 temperature). The neutral air was flushed through the chamber at different velocities, ranging from
282 0.01 to 0.05 m/s. In order to have a uniform and reliable collection of the gaseous sample at the
283 outlet, a PET tube, equipped with a sampling port, was connected to the outlet of the WT. The
284 sample was collected by means of a Nalophan® bag and a sampling vacuum pump (Capelli et al.,

285 2009). The analysis of the sample was performed by means of a GC-FID, in order to determine the
286 outlet concentration.

287 In the case of tests sets at different temperatures, the solution and the air flow were cooled down
288 or warmed up according to the temperature required for each test. To modify the temperature of
289 the air, the inlet air tube was put in a temperature-controlled bath before entering in the wind
290 tunnel. For the liquid phase, the solutions were warmed/cooled before the start, and then keep
291 constant for the duration of the trials. The temperatures tested ranged from 12°C to 42°C.

292 **3. RESULTS AND DISCUSSION**

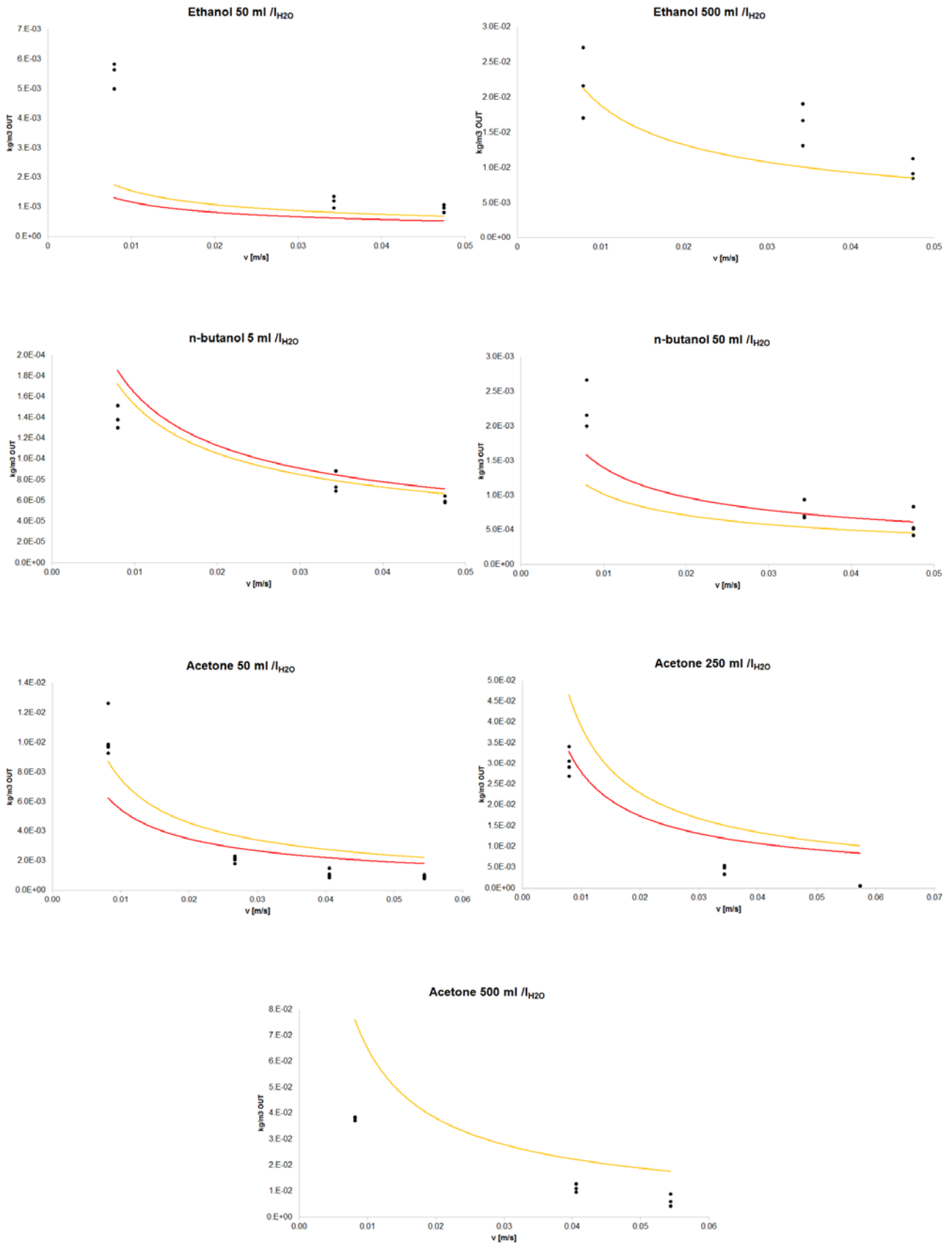
293 **3.1. Influence of velocity on volatilization at room temperature**

294 In this section, the results obtained in the experiments with dry air ($RH < 3.8\%$) are shown. For all
295 the experiments, the theoretical curve of concentration at the wind tunnel outlet was drawn as a
296 function of the air velocity inside the wind tunnel, by representing both the model proposed here
297 (dashed line), compared with the obtained experimental evaluation.

298 All the samplings were repeated, in order to evaluate the repeatability of the obtained data: the
299 black dots on the graphs report each experimental result. The ordinate reports the outlet
300 concentrations obtained for different sweep air velocity values, which in turn are reported on the
301 abscissa. The different coloured lines represent the theoretical model trends considering the two
302 approaches used to describe the interface equilibrium: the yellow one corresponds to the model
303 based on the Raoult's modified law, whereas the red one is relevant to the model based on the
304 Henry's law, as discussed in paragraph 2.1. The Henry's law trends are reported only when the
305 molar fraction of the compound is below 0.1.

306 This paragraph addresses the results of experiments in which the room temperature was
307 maintained at around 20°C . The top of Figure 4 reports the results for the ethanol solutions, at a
308 concentration of $50 \text{ mL/L}_{\text{H}_2\text{O}}$ and $500 \text{ mL/L}_{\text{H}_2\text{O}}$, in the middle the results for the n-butanol solutions,
309 respectively at $5 \text{ mL/L}_{\text{H}_2\text{O}}$ and $50 \text{ mL/L}_{\text{H}_2\text{O}}$ and in the bottom part the acetone solution trends, with
310 three different concentration of liquid solution, i.e. $50 \text{ mL/L}_{\text{H}_2\text{O}}$, $250 \text{ mL/L}_{\text{H}_2\text{O}}$ and $500 \text{ mL/L}_{\text{H}_2\text{O}}$.

311 The different concentrations used for n-butanol compared to the other compounds were chosen in
312 order to work below the solubility limit of the compound.



314

315 *Figure 4. Outlet concentration in the case of an aqueous solution of different compounds at room temperature. The*
316 *yellow line represents the results of the theoretical model based on Raoult's modified law, the red one the model based*
317 *on Henry's law evaluated only for the diluted solutions. The dots represents every measured concentration.. [2 column*
318 *fitting image]*

319 In Parker's work, two of the used compounds were classified as "gas phase controlled" (ethanol
320 and n-butanol), while acetone is reported as partially gas phase controlled, meaning that the
321 emission is a function of the velocity of the gas phase. The first studies reporting this dependence
322 in wind tunnels are those of Jiang et al. (1995), who operated their wind tunnel at high sweep air
323 velocities causing turbulent conditions inside the hood. An improvement to this was proposed by
324 Frechen et al. (2004), who first argued the necessity to operate wind tunnels at low speeds
325 (laminar conditions), in order to prevent from excessive dilution of the sampled flow.

326 The trends obtained here – using laminar conditions as in Frechen et al. (2004) - show this
327 dependence, thus being in agreement with the above mentioned studies.

328 However, it was impossible to find a unique correlation among concentration and velocity like in
329 previous studies on pure liquids (Lucernoni et al., 2017). This could be explained by the fact that
330 the present work was carried out using aqueous solutions instead of pure compounds. This entails
331 diffusive limitations also on the liquid side (and not only in the gas side as it is the case for pure
332 compounds): the air flow over the liquid surface causes the evaporation of the volatile compound at
333 the interface, thus reducing the driving force for emission. For this reason, not only the transfer
334 coefficient in the gas phase can be accounted for the explanation of the phenomenon, but also the
335 transfer coefficient in the liquid phase shall be considered, thus giving that the model becomes
336 more complex as it was the case considered by Lucernoni et al. (2017).

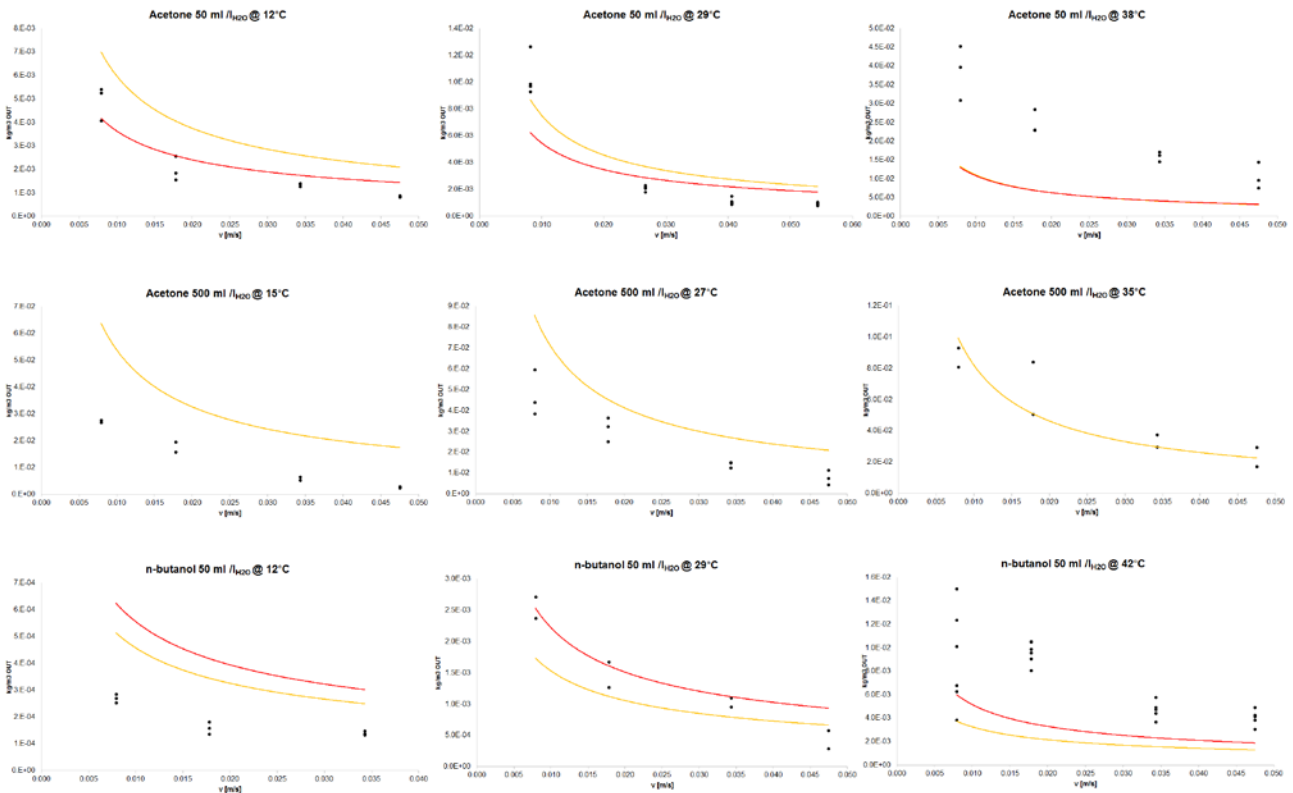
337 Further comparison with other more recent literature works is hardly done because, as previously
338 mentioned, studies dealing specifically with this problem, i.e. the dependence of the emission of
339 aqueous solutions of organic compounds inside wind tunnels from sweep air flow and temperature,
340 are limited.

341 Generally speaking, it is possible to observe a good correlation between experimental data and
342 theoretical model (a better representation for the comparison of the agreement between
343 experimental data and model is given in Figure SM2). The more important differences can be
344 found in the lowest velocities where the forced flow condition is less defined, while for the other
345 sweep air conditions the accordance is quite good.

346 **3.2. Influence of velocity on volatilization at different temperatures**

347 In order to investigate the influence of different physical parameters on volatilization, similar tests
348 were conducted by changing the temperature of the whole system. To do this, both of the two
349 contacted fluids were modified, either by heating them or by cooling them. The temperature of the
350 system was varied between 12 and 42 °C.

351 Figure 5 reports the experimental results of this test set. As in the previous case, all samplings
352 were repeated to increase the reliability of the data. The black dots indicate the experimental
353 results, while the coloured lines represent the trends of the theoretical models considered in Par.
354 2.1. In this case the trials were conducted only for acetone at two different concentrations (50
355 mL/L_{H2O} and 500 mL/L_{H2O}) and n-butanol (50 mL/L_{H2O}). The temperature of the experimental
356 system is reported over each graph.



357

358

359 *Figure 5. Outlet concentration in the case of an aqueous solution of different compounds. In this case the system once*
 360 *has been cooled and twice as been warmed. The yellow line represents the results of the theoretical model based*
 361 *Raoult's modified law, the red one the model based on Henry's law, and the dots are the measured concentrations .[2*
 362 *column fitting image]*

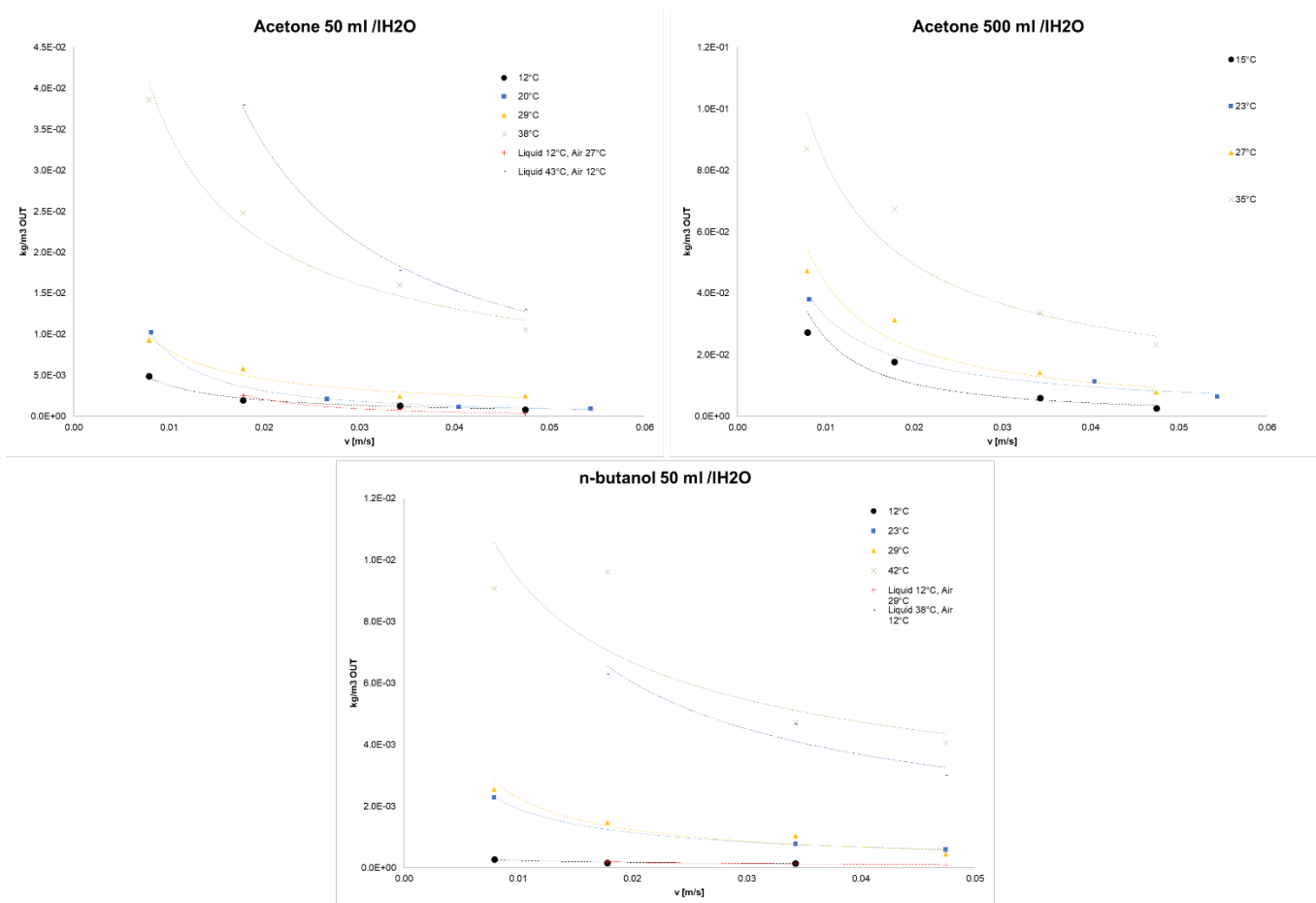
363 Also in these experiments, conducted at different temperatures, the laboratory results are in
 364 agreement with the trends of the considered theoretical model (also in this case, a better
 365 representation for the comparison of the agreement between experimental data and model is given
 366 is Figure SM3). A little deviation from the theoretical results is observed at the temperatures that
 367 are more distant from 20 °C. In particular, the theoretical model overestimates the experimental
 368 results at low temperatures, while it underestimates the trends at high temperature. This behaviour
 369 is observed both for acetone and butanol solutions. This might also be partially connected to an
 370 increased experimental error when operating at temperatures that are far from the room
 371 temperature and thus more difficult to be maintained with precision. Further investigations are
 372 needed to confirm this assumption.

373 3.3. Comparison of the effect of temperature and sweep air velocity

374 To compare the influence of the sweep air flow rate and the effect of the temperature on the
375 emission, all the trials referred to the same solution have been plotted in the same graph. Figure 6
376 reports the experimental results for the solutions of acetone at 50 ml /l_{H2O}, acetone at 500 ml /l_{H2O}
377 and n-butanol 50 at ml/L_{H2O}, respectively, at the different temperatures investigated.

378 Due to the evidence of the strong dependence of the emission on the temperature of the system, a
379 further investigation was carried out in order to verify the temperature of which side of the interface
380 (i.e. liquid or gas) has a stronger influence on the release.

381 In order to obtain this information, experiments were conducted using different temperatures for the
382 liquid and for the sweep air flow. For the diluted acetone (50 ml/L_{H2O}) two different tests were
383 conducted: one with a liquid temperature of 12°C and an inlet air temperature of 27°C, and a
384 second one with a liquid temperature of 43°C and an inlet air temperature of 12°C. For the solution
385 of n-butanolat 50 ml/L_{H2O}, a liquid temperature of 12°C and an inlet air temperature of 28°C were
386 tested, and then a liquid temperature of 38°C and an inlet air temperature of 12°C. All these
387 experimental results are reported in Figure 6.



388

389

390 *Figure 6. Experimental outlet concentrations for the solutions of acetone at 50 and 500 ml per litre and n-butanol at 50 ml*
 391 *per litre of water, at different temperatures and sweep air velocities. [2 column fitting image]*

392 Based on these results, the very strong dependence of the emitted concentration on the
 393 temperature is evident: the higher the system temperature, the higher the quantity emitted. The
 394 emission is less dependent from the sweep air flow rate at lower temperatures, while this
 395 dependence becomes stronger at high temperatures.

396 This observation is presumably connected to the trend of the vapour pressure, which grows
 397 exponentially with temperature. Therefore, even a small increase of the temperature results in a
 398 significant increase in the vapour pressure, giving that the quantity of “available” organic compound
 399 on the gas-side of the interface, which can be stripped away by the sweep air flow, is significantly
 400 increased.

401 From the results, it is also clear that the temperature of the liquid phase controls the emission and
402 not the gas phase temperature. This is also linked to the vapour pressure of the compound, which
403 is the main driving force of the phenomenon: the vapour pressure depends on the liquid
404 temperature, and the sweep air flow, due to its small heat capacity, cannot produce a significant
405 change in the liquid film temperature. For these reasons, at the interface, where chemical and
406 thermic equilibrium was assumed, the liquid side appears to control the temperature.

407 **4. CONCLUSIONS**

408 This work evaluates the effect of different variables on the emission of volatile organic compounds
409 from liquid area sources. The experiments were conducted using a wind tunnel as sampling hood.
410 A theoretical model to predict the outlet concentration of the air flow passing over the solution
411 surface is also presented.

412 Different organic compounds were used and mixed at different concentrations. In most cases the
413 proposed theoretical model predicts well the experimentally measured concentration. However,
414 some discrepancies were observed for lower velocities, where the forced flow condition is less
415 defined. Also by moving from room temperature (20° C), the theoretical model tends to
416 overestimate the experimental results at low temperatures, while it underestimates the trends at
417 high temperatures.

418 The effect of the temperature, both of the liquid solution and of the air, was investigated. The
419 temperature of the liquid significantly affects the interface evaporation and consequently the outlet
420 concentrations, while the air temperature plays a negligible role. The dependence of the outlet
421 concentration values on temperature is proven to be the same as for the interface concentration,
422 thus proving the great importance of the latter on the overall phenomenon.

423 Based on these findings, it is clear that during wind tunnel sampling the liquid temperature of the
424 area source should be taken into consideration, besides the chamber design and the sweep air
425 flow rate. This fact should be taken into account also in the legislations and norms about odour

426 sampling. Neglecting the liquid temperature variations could lead to big mistakes in the
427 experimental assessment of VOC or odour emissions from WWTPs.

428 Further studies are certainly needed to better understand the effect of humidity on the atmospheric
429 emission of different compounds from liquid solutions. In order to give an exhaustive overview, it
430 would also be interesting to investigate the behaviour to volatilization of substances having
431 different properties (e.g., very low solubility in water) from the ones here considered.

432 **ACKNOWLEDGEMENTS**

433 This research did not receive any specific grant from funding agencies in the public, commercial, or
434 not-for-profit sectors.

435

436 **BIBLIOGRAPHY**

437 Beghi, S.P., Rodrigues, A.C., Sá, L.M., Santos, J.M., 2012. Estimating hydrogen sulphide
438 emissions from an anaerobic lagoon. *Chem. Eng. Trans* 30.

439 Bianchi, A.P., Varney, M.S., 1997. Volatilisation processes in wastewater treatment plants as a
440 source of potential exposure to vocs. *Ann. Occup. Hyg.* 41, 437–454.

441 [https://doi.org/https://doi.org/10.1016/S0003-4878\(97\)00005-7](https://doi.org/https://doi.org/10.1016/S0003-4878(97)00005-7)

442 Bird, R.B., 2002. Transport phenomena. *Appl. Mech. Rev.* 55, R1--R4.

443 Bliss, P.J., Jiang, K., Schulz, T.J., 1995. The Development of a Sampling System for the
444 Determination of Odor Emission Rates from Areal Surfaces: Part II. Mathematical Model. *J.*
445 *Air Waste Manage. Assoc.* 45, 989–994. <https://doi.org/10.1080/10473289.1995.10467431>

446 Capelli, L., Sironi, S., Del Rosso, R., Céntola, P., 2009. Design and validation of a wind tunnel
447 system for odour sampling on liquid area sources. *Water Sci. Technol.* 59, 1611–1620.

448 <https://doi.org/10.2166/wst.2009.123>

449 Capelli, L., Sironi, S., Del Rosso, R., Guillot, J.-M., 2013. Measuring odours in the environment vs.
450 dispersion modelling: A review. *Atmos. Environ.* 79, 731–743.
451 <https://doi.org/10.1016/j.atmosenv.2013.07.029>

452 Carroll, J.J., 1991. What is Henry's law. *Chem. Eng. Prog.* 87, 48–52.

453 CEN, 2003. EN13725: 2003, Air quality—Determination of odor concentration by dynamic
454 olfactometry.

455 Cussler, E.L., 2009. *Diffusion: mass transfer in fluid systems*. Cambridge university press.

456 Frechen, F.B., Frey, M., Wett, M., Löser, C., 2004. Aerodynamic performance of a low-speed wind
457 tunnel. *Water Sci. Technol.* 50, 57–64.

458 Gostelow, P., Longhurst, P.J., Parsons, S., Stuetz, R.M., 2003. *Sampling for measurement of*
459 *odours*. IWA publishing.

460 Hayes, J.E., Stevenson, R.J., Stuetz, R.M., 2017. Survey of the effect of odour impact on
461 communities. *J. Environ. Manage.* 204, 349–354.
462 <https://doi.org/https://doi.org/10.1016/j.jenvman.2017.09.016>

463 Hudson, N., Ayoko, G.A., 2008. Odour sampling. 2. Comparison of physical and aerodynamic
464 characteristics of sampling devices: A review. *Bioresour. Technol.*
465 <https://doi.org/10.1016/j.biortech.2007.03.043>

466 Incropera, F.P., DeWitt, D.P., 2002. *Fundamentals of heat and mass transfer*, 5th ed. ed. J. Wiley,
467 New York.

468 Jiang, K., Bliss, P.J., Schulz, T.J., 1995. The development of a sampling system for determining
469 odor emission rates from areal surfaces: Part i. aerodynamic performance. *J. Air Waste*
470 *Manag. Assoc.* 45, 917–922. <https://doi.org/10.1080/10473289.1995.10467345>

471 Kawamura, P.I., Mackay, D., 1987. The evaporation of volatile liquids. *J. Hazard. Mater.* 15, 343–
472 364. [https://doi.org/10.1016/0304-3894\(87\)85034-3](https://doi.org/10.1016/0304-3894(87)85034-3)

- 473 Koziel, J.A., Spinhirne, J.P., Lloyd, J.D., Parker, D.B., Wright, D.W., Kuhrt, F.W., 2005. Evaluation
474 of sample recovery of malodorous livestock gases from air sampling bags, solid-phase
475 microextraction fibers, Tenax TA sorbent tubes, and sampling canisters. *J. Air Waste*
476 *Manage. Assoc.* 55, 1147–1157.
477 <https://doi.org/https://doi.org/10.1080/10473289.2005.10464711>
- 478 Laska, M., Hudson, R., 1991. A comparison of the detection thresholds of odour mixtures and their
479 components. *Chem. Senses* 16, 651–662. <https://doi.org/10.1093/chemse/16.6.651>
- 480 Leonardos, G., Kendall, D., Barnard, N., 1969. Odor Threshold Determinations of 53 Odorant
481 Chemicals. *J. Air Pollut. Control Assoc.* 19, 91–95.
482 <https://doi.org/10.1080/00022470.1969.10466465>
- 483 Liss, P.S., Slater, P.G., 1974. Flux of Gases across the Air-Sea Interface. *Nature* 247, 181.
- 484 Lucernoni, F., Capelli, L., Busini, V., Sironi, S., 2017. A model to relate wind tunnel measurements
485 to open field odorant emissions from liquid area sources. *Atmos. Environ.* 157, 10–17.
486 <https://doi.org/10.1016/j.atmosenv.2017.03.004>
- 487 Montes, F., Hafner, S.D., Rotz, C.A., Mitloehner, F.M., 2010. Temperature and air velocity effects
488 on ethanol emission from corn silage with the characteristics of an exposed silo face. *Atmos.*
489 *Environ.* 44, 1987–1995. <https://doi.org/https://doi.org/10.1016/j.atmosenv.2010.02.037>
- 490 Parker, D.B., Caraway, E.A., Rhoades, M.B., Cole, N.A., Todd, R.W., Casey, K.D., 2010. Effect of
491 Wind Tunnel Air Velocity on VOC Flux from Standard Solutions and CAFO
492 Manure/Wastewater. *Trans. ASABE*.
- 493 Prata A.A., J., Santos, J.M., Timchenko, V., Stuetz, R.M., 2018. A critical review on liquid-gas
494 mass transfer models for estimating gaseous emissions from passive liquid surfaces in
495 wastewater treatment plants. *Water Res.* 130, 388–406.
496 <https://doi.org/10.1016/j.watres.2017.12.001>
- 497 Prata, A.A., Santos, J.M., Timchenko, V., Reis, N.C., Stuetz, R.M., 2017. Wind friction

498 parametrisation used in emission models for wastewater treatment plants: A critical review.
499 Water Res. 124, 49–66. <https://doi.org/https://doi.org/10.1016/j.watres.2017.07.030>

500 Raimundo, A.M., Gaspar, A.R., Oliveira, A.V.M., Quintela, D.A., 2014. Wind tunnel measurements
501 and numerical simulations of water evaporation in forced convection airflow. Int. J. Therm.
502 Sci. 86, 28–40. <https://doi.org/https://doi.org/10.1016/j.ijthermalsci.2014.06.026>

503 Ryden, J.C., Lockyer, D.R., 1985. Evaluation of a system of wind tunnels for field studies of
504 ammonia loss from grassland through volatilisation. J. Sci. Food Agric. 36, 781–788.
505 <https://doi.org/https://doi.org/10.1002/jsfa.2740360904>

506 Sander, R., 2015. Compilation of Henry's law constants (version 4.0) for water as solvent. Atmos.
507 Chem. Phys. 15, 4399–4981. <https://doi.org/10.5194/acp-15-4399-2015>

508 Schiffman, S.S., Miller, E.A.S., Suggs, M.S., Graham, B.G., 1995. The effect of environmental
509 odors emanating from commercial swine operations on the mood of nearby residents. Brain
510 Res. Bull. 37, 369–375. [https://doi.org/https://doi.org/10.1016/0361-9230\(95\)00015-1](https://doi.org/https://doi.org/10.1016/0361-9230(95)00015-1)

511 Smith, F.L., Harvey, A.H., others, 2007. Avoid common pitfalls when using Henry's law. Chem.
512 Eng. Prog. 103, 33–39.

513 Smith, R.J., Watts, P.J., 1994. Determination of Odour Emission Rates from Cattle Feedlots: Part
514 2, Evaluation of Two Wind Tunnels of Different Size. J. Agric. Eng. Res. 58, 231–240.
515 <https://doi.org/https://doi.org/10.1006/jaer.1994.1053>

516 Sutton, O.G., 1934. Wind structure and evaporation in a turbulent atmosphere. Proc. R. Soc. Lond.
517 A 146, 701–722.

518 Thibodeaux, L.J., Mackay, D., 2010. Handbook of chemical mass transport in the environment.
519 CRC Press.

520 Van Harreveld, A.P., 2001. From odorant formation to odour nuisance: new definitions for
521 discussing a complex process. Water Sci. Technol. 44, 9–15.

522 Whitman, W.G., 1962. The two film theory of gas absorption. *Int. J. Heat Mass Transf.* 5, 429–433.
523 [https://doi.org/https://doi.org/10.1016/0017-9310\(62\)90032-7](https://doi.org/https://doi.org/10.1016/0017-9310(62)90032-7)

524 Yuwono, A.S., Lammers, P.S., 2004. Odor pollution in the environment and the detection
525 instrumentation. *Agric. Eng. Int. CIGR J.*

526 Zuend, A., Marcolli, C., Booth, A.M., Lienhard, D.M., Soonsin, V., Krieger, U.K., Topping, D.O.,
527 McFiggans, G., Peter, T., Seinfeld, J.H., 2011. New and extended parameterization of the
528 thermodynamic model AIOMFAC: calculation of activity coefficients for organic-inorganic
529 mixtures containing carboxyl, hydroxyl, carbonyl, ether, ester, alkenyl, alkyl, and aromatic
530 functional groups. *Atmos. Chem. Phys.* 11, 9155–9206.

531